

This discussion paper is/has been under review for the journal Solid Earth (SE).  
Please refer to the corresponding final paper in SE if available.

# The European Alps as an interrupter of the Earth's conductivity structures

D. Al-Halbouni<sup>1,\*</sup>

<sup>1</sup>Institute of Geophysics, University of Göttingen, Friedrich-Hund-Platz 1, 37077 Göttingen, Germany

\* now at: Instituto Dom Luíz, Faculdade de Ciências, University of Lisbon, Campo Grande edifício C8 piso 3, 1749-016 Lisboa, Portugal

Received: 23 June 2013 – Accepted: 8 July 2013 – Published: 17 July 2013

Correspondence to: D. Al-Halbouni (dj.alhal@gmx.de)

Published by Copernicus Publications on behalf of the European Geosciences Union.

Title Page

Abstract

Introduction

Conclusions

References

Tables

Figures

⏪

⏩

◀

▶

Back

Close

Full Screen / Esc

Printer-friendly Version

Interactive Discussion



## Abstract

Joint interpretation of magnetotelluric and geomagnetic depth sounding results in the period range of  $10\text{--}10^5$  s in the Western European Alps offer new insights into the conductivity structure of the Earth's crust and mantle. This first large scale electromagnetic study in the Alps covers a cross-section from Germany to northern Italy and shows the importance of the alpine mountain chain as an interrupter of continuous conductors. Poor data quality due to the highly crystalline underground is overcome by Remote Reference and Robust Processing techniques and the combination of both electromagnetic methods. 3-D forward modeling reveals on the one hand interrupted dipping crustal conductors with maximum conductances of 4960 S and on the other hand a lithosphere thickening up to 208 km beneath the central Western Alps. Graphite networks arising from Palaeozoic sedimentary deposits are considered to be accountable for the occurrence of high conductivity and the distribution pattern of crustal conductors. The influence of huge sedimentary Molasse basins on the electromagnetic data is suggested to be minor compared with the influence of crustal conductors. Dipping direction (S–SE) and maximum angle ( $10.1^\circ$ ) of the northern crustal conductor reveal the main thrusting conditions beneath the Helvetic Alps whereas the existence of a crustal conductor in the Briançonnais supports theses about its belonging to the Iberian Peninsula. In conclusion the proposed model arisen from combined 3-D modeling of noise corrected electromagnetic data is able to explain the geophysical influence of various structural features in and around the Western European Alps and serves as a background for further upcoming studies.

## 1 Introduction

The European Alps are regarded as the junction between the European and African continent. Its multifarious geology and geological development is still part of intensive scientific research in Europe. Numerous geological works lead to the nowadays widely

SED

5, 1031–1079, 2013

## Alps conductivity

D. Al-Halbouni

Title Page

Abstract

Introduction

Conclusions

References

Tables

Figures

⏪

⏩

◀

▶

Back

Close

Full Screen / Esc

Printer-friendly Version

Interactive Discussion



## Alps conductivity

D. Al-Halbouni

Title Page

Abstract

Introduction

Conclusions

References

Tables

Figures

⏪

⏩

◀

▶

Back

Close

Full Screen / Esc

Printer-friendly Version

Interactive Discussion



accepted basic structuring of the Alps as stacked nappes of the Helvetic, Penninic, Aus-  
 troalpine and Southern Alps (Fig. 1). For investigation of greater depths nowadays basi-  
 cally seismic methods are used and show in essence a northern dipping European con-  
 tinental margin, overthrusting of crystalline massifs as well as rests of oceanic crust and  
 the Adriatic plate (Schmid and Kissling, 2000). The asthenosphere lies therefore much  
 deeper ( $> 200$  km) than in the remaining Phanerozoic Europe (Jones et al., 2010). In  
 general the lithosphere-asthenosphere boundary (LAB) is referred to as a limit between  
 rigid material and ductile material in the Earth's mantle (Jones et al., 2010). There exist  
 numerous definitions of the LAB depending on which physical properties (e.g. seismic  
 velocities, chemical composition, thermal structure) are observed (Artemieva, 2009).  
 In this study we refer to the LAB defined by electromagnetics, e.g. a sharp increase in  
 conductivity with depths.

In contrast to the quantity of seismic measurements in the Alps there is a lack of  
 other geophysical methods. Especially electromagnetic investigation in the European  
 Alps have been scarcely performed in the last decades although the quality of the  
 techniques is comparably high and analysis of local or widespread, shallow or deep 3-D  
 structures is nowadays standard. One reason for this discrepancy lies in the presence  
 of high levels of anthropogenic noise. Many of the studies either remained focused on  
 local noise-free areas or could not meet the requirements of reproducible data. This  
 work uses today's well developed noise reducing methods and provides with this help  
 a first large scale study of the conductivity in the Western Alps.

Electrically highly conductive structures in the Earth's crust and mantle exist in many  
 parts of middle and southern Europe (Korja, 2007). In Germany e.g. there exists geo-  
 physical evidence of conductors in the regions of the Rhenish Massif (Leibecker et al.,  
 2002) and especially beneath the Black Forest and the Rhine Graben north of the Euro-  
 pean Alps (see e.g. Schmucker and Tezkan, 1988). Former works of Kemmerle (1977)  
 in the Eastern Alps and Bahr (1993) in the Western Alps provide suggestions about  
 the interruption of such conductive structures beneath the mountain chain. Contrary  
 to these findings Schnegg (1998) and Gurk (2000) prove the existence of a crustal

conductor in the Penninic Alps. All these works have in common the focus on certain local areas and the missing integration of a possible cause of high conductivity into the geological-tectonic background.

With the following work we present a study about the interruption of conductive structures in the Western mountain chain. Focused on a large scale, this survey is aimed to investigate the deep conductivity structure of the Earth and its relation to the alpine tectonic background. We overcome the problem of anthropogenic noise for a fair deal with the combination of two different electromagnetic methods and the substantial application of processing techniques. For this first study traversing the Alps from the Black Forest (Germany) to the Po basin (Italy) magnetotelluric (MT) and geomagnetic depth sounding (GDS) data was collected in 2008/2009 along a 330 km cross-section (Fig. 1). The application of Remote Reference and Robust Processing techniques (Egbert and Booker, 1986) prove to be successful to enhance data quality. The combination of MT and GDS serves as a way to manage data quality limits and gaps. It hence enables a more complete insight into the conductivity structure along the profile, enabling studies both of the crust as well as the mantle.

Large scale geological features in and around the European Alps like the Rhine, Rhône and Bresse Graben, the Mediterranean Sea as well as the tertiary Molasse basins (see Fig. 1) play an important role regarding their influence on the flow and distribution of electric currents. An estimation of their relevance in comparison to deeper crustal conductivity structures is provided in the modeling section. At the same time the different tectonic regimes of the Alps are taken into account. To avoid underestimation of the dimensionality effects of lateral heterogeneities a key point here is the use of 3-D forward modeling that proves to be adequate although the profile might suggest a 2-D interpretation.

A main point of this study focusses on the crustal structures of the first 25 km depth and their evolution along the cross-section. High conductivity structures that were found with previous electromagnetic studies in and around the Alps are analyzed, partially reinvestigated and reliable findings are included as pre conditioning in the modeling.

## SED

5, 1031–1079, 2013

### Alps conductivity

D. Al-Halbouni

Title Page

Abstract

Introduction

Conclusions

References

Tables

Figures

◀

▶

◀

▶

Back

Close

Full Screen / Esc

Printer-friendly Version

Interactive Discussion



**Alps conductivity**

D. Al-Halbouni

Title Page

Abstract

Introduction

Conclusions

References

Tables

Figures

I◀

▶I

◀

▶

Back

Close

Full Screen / Esc

Printer-friendly Version

Interactive Discussion



The calculated MT transfer functions build the fundament to find out the conductivity distribution with depth which is used as a realistic basis for GDS transfer functions. GDS offers additional data without extra costs and shows to be necessary for a reliable modeling in such an electromagnetically disturbed environment. Although the disturbances lead to a lack of electric data in some cases, longer periods of the undisturbed stations can be used to determine the conductivity structure of the Earth's mantle.

A general three dimensional model has been developed to explain the gross of electromagnetic data achieved in this study. Several restrictions of the joint modeling of GDS and MT results have been found and emphasized (Sect. 4.4). The general model nevertheless shows a reasonable explication for the resistivity distribution underneath the Western European Alps. It constitutes a first model for this area and its broad surrounding and is presented in Sect. 4.1. The steps of introducing a dipping crustal conductor and its interruption north and west of the mountain chain prove to be essential to explain the obtained electromagnetic data.

A discussion of the possible causes of high conductivities and its heterogenic distribution as well as interruption is provided in the following Sect. 5. As the findings of this investigation offer completely new insights into the conductivity structure of the European Alps, Sect. 6 deals with possible geotectonic explanations. A connection to the orogenic background of the Alps and an outlook to future projects and deeper investigation are given in the last part. It is shown that there is an existential relationship between the distribution of geological units in Earth's history, the heterogene distribution of crustal conductors and the existence of graphite.

## 2 Material and methods

### 2.1 Physical background

Electromagnetic depth sounding offers a cost-effective possibility to investigate the Earth's conductivity structure with high resolution. On the one hand it includes mag-

netotellurics (Tikhonov, 1950; Cagniard, 1953), a passive induction method using the frequency–dependent relation between electric ( $E$ ) and magnetic fields ( $B$ ) measured at the surface. Herewith the impedance  $Z$  of the Earth’s interior structures is determined according to the relationship

$$E = Z \cdot B. \quad (1)$$

The apparent resistivity ( $\rho_a$ ) is linked to the impedance by  $\rho_a = \mu_0 |Z|^2 / \omega$  with ( $\omega$ ) as the angular frequency and ( $\mu_0$ ) the magnetic permeability of free space. Because small-scale scatterers impose static shift on the amplitude of the impedance but do not affect the phase ( $\phi = \arctan(\Im Z / \Re Z)$ ) (Groom and Bahr, 1992; Caldwell et al., 2004; Simpson and Bahr, 2005), only the latter is used for interpretation and modeling of the MT part in this study. Both parameters are connected via a Kramers–Kronig dispersion relationship (Weidelt, 1972). The anisotropy factor  $A = \sqrt{\rho_{\perp} / \rho_{\parallel}}$  is calculated using the resistivity values perpendicular ( $\rho_{\perp}$ ) and parallel ( $\rho_{\parallel}$ ) to the strike direction of modeled lamellas (Eisel and Haak, 1999). The phase sensitive strike angle  $\alpha$  is determined by the minimization of phase differences (see e.g. Bahr, 1988, 1991; Groom and Bahr, 1992; Jones and Groom, 1993; Caldwell et al., 2004) and is referred to as electromagnetic strike in this study.

On the other hand we used the geomagnetic depth sounding method (Schmucker, 1970), which compares magnetic fields at different locations using the frequency-dependent perturbation tensor  $W$  according to

$$B^a = W \cdot B^{\text{ref}} = \begin{pmatrix} h_H & h_D \\ d_H & d_D \\ z_H & z_D \end{pmatrix} \cdot \begin{pmatrix} B_x^{\text{ref}} \\ B_y^{\text{ref}} \end{pmatrix}, \quad (2)$$

where  $B^a$  is the anomalous and  $B^{\text{ref}}$  the reference magnetic field. In this study the dimensionless horizontal transfer functions  $h_H$  and  $d_D$  are relevant whereas  $h_D$  and  $d_H$  tend to equal zero for all periods. Anomal currents arise in areas with high variation

Title Page

Abstract

Introduction

Conclusions

References

Tables

Figures

⏪

⏩

◀

▶

Back

Close

Full Screen / Esc

Printer-friendly Version

Interactive Discussion



## Alps conductivity

D. Al-Halbouni

Title Page

Abstract

Introduction

Conclusions

References

Tables

Figures

⏪

⏩

◀

▶

Back

Close

Full Screen / Esc

Printer-friendly Version

Interactive Discussion



from an 1-D conductivity underground and lead to a complete impedance- and GDS-tensor. Lateral conductivity changes produce local vertical magnetic fields ( $B_z$ ) whose relation to the horizontal fields at one station are described according to the formula that relates the local magnetic field vector entries ( $B_x$  and  $B_y$ ) (Parkinson, 1959; Wiese, 1962)

$$B_z = z_H' B_x + z_D' B_y. \quad (3)$$

This local induction, marked by the superscript /, can be used to trace a preferred flow of electric currents and therefore indicates macro-anisotropic structures.  $z_H'$  and  $z_D'$  are the dimensionless local vertical magnetic transfer functions.

## 2.2 Equipment and data collection

Up to seven stations recording electric and magnetic fields during 6 months in winter and spring of 2008/2009 were deployed along the 330 km long cross-section (Fig. 1). Data was recorded with a sampling rate of 2–4 s using the RAP-system developed at the University of Göttingen. It consists of a robust 16-bit datalogger with telluric and magnetic amplifiers, a triaxial fluxgate magnetometer and four Ag–AgCl electrodes. Depending on the terrain conditions, the installation of the electrodes followed either a shape of a cross, or a L-shape using one common electrode for the N-S and E-W component. The device was supplied by three 12 V batteries which are able to resist up to four weeks in such a cold mountaineous environment (down to  $-20^\circ\text{C}$  at altitudes up to 1100 m). Temperature effects on the data recording system could be completely avoided due to the fact that snow cover worked like insulating layers and a deep bury of the electrodes and magnetometers (Fig. D1).

## 2.3 Processing methods

Different approaches to cope with the unavoidable anthropogenic noise in the logistically challenging mountain chain proved to be successful. Before recording, the careful

selection of remote areas and the observation of not only test data but also test spectra (like shown in Fig. B1a) are important to verify the presence of noise frequencies. In detail the following steps have been undergone to improve data quality after recording:

1. Selection of undisturbed data sets, e.g. focus on daytime data or magnetically active days.
2. Robust Processing (Egbert and Booker, 1986) of electric and magnetic data which removes outliers from the spectra.
3. The use of a magnetic Remote Reference station to diminish the effect of coherent noise in the spectra.

DC railways in Italy are the most displeasing interferers for MT-measurements (Larsen et al., 1995), generally leading to electric currents flowing tens of kilometers in highly crystalline underground (Pádua et al., 2002). The problem in point one mentioned above is the loss of longer periods due to data cutting off. Bearing these issues in mind, the northernmost station WOLF (Fig. 1) with the best data quality is used both as the GDS and Remote Reference site. The latter combined with Robust Processing (Egbert and Booker, 1986) of up to 4 iterations yielded reliable results and an increase of the analyzable period-range for some of the disturbed stations (Fig. B1b). Even though a careful selection and data improvement process has been pursued, electric data of stations built directly on crystalline ground (in this case MALE, CERV, VALG) could not be recovered due to the high electric railway noise. This is the point where recording of the generally less disturbed magnetic data and the use of the GDS method is essential for further investigation and construction of a continuous model (see Sect. 4.1). The applied processing methods of Remote Reference proved to be successful even at the strongly disturbed southernmost station BORG. Looking at the spectra of this station (exemplary  $E_x$  in Fig. A1) one cannot deduce whether it is natural or artificial, so the influence of expected disturbing frequencies in the Po basin seems to be hidden with the same amplitude like natural signals. Nevertheless a closer look at the MT sounding

Title Page

Abstract

Introduction

Conclusions

References

Tables

Figures

◀

▶

◀

▶

Back

Close

Full Screen / Esc

Printer-friendly Version

Interactive Discussion



curve reveals it to be similar to Controlled Source MT curves (Routh and Oldenburg, 1999) mainly influenced by highly coherent noise, with a phase drop to nearly 0° and a 45° rise of the apparent resistivity in a log-log plot (Fig. B1a). The applied magnetic Remote Reference with WOLF can finally achieve reliable results for nearly half of the investigated periods.

The magnetic influence of railways diminishes in a few kilometers distance (Szarka, 1988), concentrated on the  $B_z$ -component (see Fig. B2) and therefore leads to unaffected horizontal magnetic components. The combination of MT and GDS hereby increases the amount of usable data significantly. It not only fills the data-gaps due to the variance of anthropogenic noise but also affords advantages in spatial resolution. MT hereby is essential to determine conductivity characteristics at the reference site so that GDS has a reliable basis.

### 3 3-D forward modeling

#### 3.1 Model composition

After processing the noise-corrected data is then used to determine the physical quantities mentioned in Sect. 2.1 necessary for modeling (MT-phases, geomagnetic transfer functions and local magnetic field vector entries). The apparent resistivity has not been used as a parameter because of the high influence of static shift in this rangy and highly heterogeneous terrain (see Sect. 2.1) and the missing reliable estimation of static shift factors.

The measurement stations lie basically on a cross-section from N to S with a maximum of 25 km distance perpendicular to an imaginary line. This arrangement might suggest a 2-D interpretation of the results but during the modeling 1-D or 2-D structures appeared to be insufficient to explain the data. More precisely the lateral heterogeneities of the Alps and its surroundings need a 3-D model. Because GDS and MT are volume sounding methods both are very susceptible for lateral resistivity variations.

Title Page

Abstract

Introduction

Conclusions

References

Tables

Figures



Back

Close

Full Screen / Esc

Printer-friendly Version

Interactive Discussion





## Alps conductivity

D. Al-Halbouni

Title Page

Abstract

Introduction

Conclusions

References

Tables

Figures

I◀

▶I

◀

▶

Back

Close

Full Screen / Esc

Printer-friendly Version

Interactive Discussion



5  
10  
15  
20  
25

tion is not necessary (see Figs. 3 and 4), as the main influence on the characteristic electromagnetic data of this study comes from higher conductive structures embedded in a resistive background. The geologic background of the European Alps is therefore basically used for the initial definition of ranges, geometrical limits and boundaries, but due to its superficial character the model was independently and successively developed. Influence of several well-known geologic features around and inside the Alps (like the Molasse basin and structures with proposed geomagnetic influence like the *Bündnerschiefer*, compare Gurk and Schnegg, 2001; Gurk, 1999). is tested by inclusion in the model. As described in the following Sect. 4.2, an agreement between some modeled structures and their geologic counterparts with their continuation into deeper layers is in fact observed at some crucial areas.

## 4 Results

### 4.1 Overview

15  
20  
25

3-D forward modeling allowed to achieve the final model presented in Figs. 3 and 4, explaining both the GDS and partially MT results in a period-range between 10 and  $10^5$  s along the cross-section.<sup>1</sup> The core, the most influential part of the model, is presented in Fig. 3 whereas Fig. 4 indicates the structures along a 2-D cross-section following the approximate positions of the stations. The modeled parameters are on the one hand the GDS tensor elements  $h_H$  and  $d_D$ , while on the other hand the MT phases  $\phi_{xy}$  and  $\phi_{yx}$  as well as partially the local induction  $z_D$  are considered. The apparent resistivity data is not taken into account because of high static shift in the mountain zones emerging from local anomalies. It is not the intention to model the static shift or correct it because the phases offer sufficient information (compare Sect. 2.1 and Caldwell et al., 2004). For completion the whole impedance tensor elements of the seven stations are shown in Figs. C1 to C4.

<sup>1</sup>The original data is available at doi:10.1594/PANGAEA.770504.

## 4.2 Data fit of model structures

- The Rhine Graben west of the Black-Forest is the most important geological feature filled with highly conductive tertiary sediments up to 3.35 km thickness (Illies, 1972). The high values of local induction  $z_D$  (see Sect. 2) arising consequently at the reference station WOLF are compensated by the existence of a high conductive crustal structure (Fig. 5). Using phase-trends and horizontal magnetic transfer functions along the whole cross-section its depth at the reference station is modeled at 5–7 km with a conductance of  $\tau = 4960$  S, which is higher and shallower than previous results (Tezkan et al., 1992; Schmucker and Tezkan, 1988). These findings build the basis for the interpretation of crustal anomalies with reference to WOLF. The characteristic ascending trend of phase-curves for longer periods reveal a conductive upper mantle zone from 86 km beneath the Black Forest (Figs. 6 and 7) with a conductance of 6440 S according to the 3-D forward modeling.
- In contrast in the central Western Alps (beneath the Helvetic and Penninic domains, see Fig. 1) the effect appears at higher periods (Fig. 8) and is reproduced by a conductive zone of 4000 S starting in depths of 208 km. South of the Alps its effect again appears in shorter periods. This leads to the conclusion of a deeper LAB beneath the central part of the Western European Alps compared to the rest of western and central Europe. Typical conductivity values for the asthenosphere underneath continents are between  $0.01 - 0.1 \text{ Sm}^{-1}$  (Heinson, 1999). This study therefore additionally fills an important gap in the data for statistical estimation of the electromagnetic LAB (Jones et al., 2010). The values derived in this study, from  $0.012 \text{ Sm}^{-1}$  beneath the Black Forest up to  $0.02 \text{ Sm}^{-1}$  beneath the Alps agree to the above mentioned range under continental plates.
- From 408 km depth a resistivity of  $15 \Omega\text{m}$  is inferred from the MT by reproducing the long period phase data.

## Alps conductivity

D. Al-Halbouni

Title Page

Abstract

Introduction

Conclusions

References

Tables

Figures

I◀

▶I

◀

▶

Back

Close

Full Screen / Esc

Printer-friendly Version

Interactive Discussion



- The top of the model consists of a 500 m thick layer with  $\rho = 20 \Omega\text{m}$ . It cannot be attributed to a geological layer all over the study area, although in some parts one can compare it to young sedimentary cover and rocks with higher conductivity (e.g. by groundwater or alteration). It is introduced to rise the phases (see e.g. Figs. 6 and 7) at short periods as required by the data.
- The effect of the Mediterranean Sea<sup>2</sup> (MS in Figs. 3 and 4) especially on the southernmost station BORG is investigated and taken into account in the final model. The sea has been modeled with a resistivity of  $0.3 \Omega\text{m}$  up to depths of 2.6 km according to recent bathymetry datasets (Medimap Group, 2005) and a sedimentary layer with  $50 \Omega\text{m}$  beneath. The conductance of the seawater is therefore around  $3.33 \text{Sm}^{-1}$ , a typical value chosen for water of mean salinity (Simpson and Bahr, 2005). Although this value could be too low for the Mediterranean Sea (Simpson and Tommasi, 2005), the so-called coast effect, the influence of deviated current (see Parkinson, 1959; Monteiro et al., 2001), is not expected to have considerably more than the observed marginal influence on long periods (here  $> 300 \text{s}$ ) as the location of the last station of the cross-section has been chosen far away from the continental margin. The comparison between the final model and the data of BORG are given in Fig. 9. Even though we used detailed data processing techniques the errors of both phase polarizations are high and the model gives a finally insufficient fit which could be improved by relocating the station.
- The transition zone between the northern alpine foreland is dominated by the Molasse basin, filled with synorogeous conductive sediments. We apply a step-wise approximation to model the dipping Molasse and crustal conductor as seen in Fig. 4 and achieve results perfectly fitting with the observed ones at the relevant

<sup>2</sup>Explicitly the Ligurian Sea in this study.

Title Page

Abstract

Introduction

Conclusions

References

Tables

Figures

◀

▶

◀

▶

Back

Close

Full Screen / Esc

Printer-friendly Version

Interactive Discussion



station INNT<sup>3</sup> in the Valais (Fig. 8). In the model thicknesses of up to 7 km and conductances up to 1400 S prove to be adequate. The best reproduction of MT-phases, phase-splits and GDS transfer functions is achieved by introducing S-SE dipping structures.

5 **4.3 The importance of GDS**

GDS is found to be the most appropriate method to receive information especially about the Earth’s crust. The key point concerning the GDS transfer functions (see Sect. 2) at all periods is a continuous decrease of  $d_D$  from N to S along the cross-section and a minimum of  $h_H$  in the area between Valgrande and Valsesia (Figs. 10 and 11); the effect is mostly seen at the periods 128 s and 256 s.

The model is able to explain all GDS values we are interested in (Figs. 10 and 11) based on three important features:

1. The first point is the interruption of the northern, at maximum 10.1° S–SE dipping crustal conductor (C1) in depths around 13 km beneath the Helvetic zones of the Alps giving rise to the characteristic course of  $h_H$ . The Po basin with a highest conductance of 1800 S hereby plays an important role to the renewed ascent.
2. In second place a very conductive, at maximum 37.2° SE dipping structure is necessary in the Briançonnais zone to reproduce the  $d_D$  values, confirming former results of a local study in the Penninic Alps (Schneegg, 1998). The conductance of this structure in depths just before the interruption occurs (13 km) is around 8060 S.
3. All effects are modulated by the existence of the SE–E dipping crustal conductor on the western side of the mountains, necessary to explain GDS effects of

<sup>3</sup>INNT has been located very close to a former station URBA from Bahr et al. (1993) to confirm and reassess its data.

Title Page

Abstract

Introduction

Conclusions

References

Tables

Figures



Back

Close

Full Screen / Esc

Printer-friendly Version

Interactive Discussion



INNT. According to the proposed existence of conductive structures in the crust of central Europe due to several MT-studies (see Gatzemeier and Moorkamp, 2005; Tezkan et al., 1992, and references within) a simplified continuation of this layer is adopted.

5 **4.4 Model robustness and restrictions**

The importance of all structures included in the final model and their parameters is tested in several hundred 3-D forward models. In this paper the most important part is shown. Despite the low number of stations (Fig. 1), with the help of the high horizontal resolution of GDS, 3-D forward modeling of structures lying beside the N-S line is necessarily performed to explain the data. Comparison of data and model results is shown in Figs. 5 to 11. The purpose of the comparison is to highlight the importance of certain conductors like the crustal conductor (C1), the Molasse (NM), the Briançonnais conductor (C2) and the mantle conductor (MC). The effect of the structures is often limited to certain periods so that a whole set of GDS results from 128–1024 s is shown in Figs. 10 and 11. The C1 proves to be necessary in all periods to achieve a correct trend of the GDS-tensor whereas the MC only affects lower frequencies (see Fig. 11c and d). The Molasse and C2 are regionally necessary and in fact the final model emerges out of the best possible combination of plenty of models and represents the best fit in many cases, although a perfect fit to the observed data can often not be achieved, leaving gaps of up to 0.1. Modeling code restrictions impede including higher conductivity variations between adjacent layers (Mackie and Booker, 1999) which could probably improve the fit.

Attention must be drawn to remaining spatial aliasing. No station was located in the northern Molasse basin, where a maximum of  $h_H$  must occur according to a 2-D xy-slice of the modeled results (not shown in this publication).

Additionally an important restriction must be mentioned at this point. The model must contain at the same time a high resolution for short periods and a large dimension to fulfill long periods and the nature of the N–S cross-section. Due to the fact that only

## Alps conductivity

D. Al-Halbouni

Title Page

Abstract

Introduction

Conclusions

References

Tables

Figures

◀

▶

◀

▶

Back

Close

Full Screen / Esc

Printer-friendly Version

Interactive Discussion



macroscopic anisotropy (see Sect. 2) can be used in the 3-D forward modeling code (Mackie and Booker, 1999), fulfilling both requirements is not possible. The focus in this case was the establishment of a regional model explaining the gross of EM data in the Western Alps. Data from the Black Forest (stations WOLF and HAEN, see Fig. 1) show an anisotropic crustal conductor, assessed by local induction studies (Fig. 5). This fact has been recognized but not included in the figure of the final model (Fig. 3). In general, although an N–S interrupted anisotropic C1 with the same apparent resistivity in N–S direction like an isotropic C1 should have the same effect on  $h_H$ , the 3-D forward model does not show this. Instead, a much lower interruption effect appears. In our case the whole effect of an interrupted conductor nearly disappears when including anisotropy and the course of the diagonal GDS tensor elements cannot be reproduced. GDS features would basically follow the huge lamellae used to model anisotropy macroscopically. As explained above, a denser modeling grid could on the one hand avoid these problems but on the other hand impede a large scale model. As a solution the anisotropy is not considered in the final model explaining GDS data (Figs. 3, 10 and 11), but nevertheless when looking at MT curves in the Black Forest, anisotropy must be included.

If an anisotropy of  $A = 1.41$  is appointed to the C1, with a higher conductivity in the electromagnetic strike direction of  $\alpha \sim N 30^\circ E$  for short periods (Fig. 12), then the model is able to explain MT data in the Black Forest as seen in Figs. 6 and 7. The same observations count for the mantle conductor beneath the Black Forest. The MT data requires a higher conductive mantle in E–W direction ( $A = 1.73$ ) with an electromagnetic strike direction of  $\alpha \sim N 80\text{--}90^\circ E$  (Fig. 12). Instead for station INNT in the Alps an anisotropic mantle is not needed anymore to reproduce the data (Fig. 8), the phase split occurs only due to the dipping of the structures. However this leaves room for the possible existence of anisotropy in C1 underneath INNT but with a lower (and not resolvable) extent. Further and dense investigation in this area is needed to clarify these restrictions.

## 5 Discussion

The model in Fig. 3 represents a good explanation regarding large scale EM data along a huge part of the Western Alps. Due to the nature of 3-D forward modeling of long period data the results go beyond a simple 2-D modeling along the cross section and can be proved or modified in further studies. The general fact that can be deduced from the modeling results is that the interruption of crustal conductors in the Western European Alps is able to explain the large scale effects on GDS and MT data. Additional effects of the huge sedimentary basins around the Alps, the Rhine Graben as well as the regional Briançonnais conductor are taken into account and confirm their influence. The picture is completed by new information about the mantle conductor and its interruption. The difficulty in determining possible anisotropy is attributed in general to the restrictions of the modeling code regarding GDS parameters. Nevertheless separate modeling of MT and GDS gives indications about anisotropic zones. The electric data quality in general must be evaluated as bad in the southern part of the Western Alps so that the model fit to MT phases is not accurate enough in that area. Further studies in those areas should take that into account and locate the stations basically on sedimentary basins, even though the static shift effect is likely to be high there.

Discussion still goes on about the nature of the crustal conductor. High conductivity can be attributed amongst others to saliniferous fluids, partial melts or graphite (Simpson, 1999; Nover et al., 2005; Schwarz, 1990). Although strongly debated (Wanamaker, 2000) and refused by e.g. Yardley and Valley (1997), the latter is regarded to be the principal cause in this case due to the following simple observations. With the fluid model, the conductivities found around  $2 \text{ S m}^{-1}$  could only be achieved by unrealistic high volume fractions (at least 15% of saliniferous fluids) whereas yet 0.003% of perfectly connected graphite suffices for the Hashin–Shtrikman upper bound, the upper limit of an effective conductivity in a 2-phase medium (Waff, 1974). The conductance in deeper dipped structures rises even though porosity will decline, so that fluids are unlikely to be the cause. A key feature in and around the Alps is the heteroge-

SED

5, 1031–1079, 2013

### Alps conductivity

D. Al-Halbouni

Title Page

Abstract

Introduction

Conclusions

References

Tables

Figures

⏪

⏩

◀

▶

Back

Close

Full Screen / Esc

Printer-friendly Version

Interactive Discussion



**Alps conductivity**

D. Al-Halbouni

Title Page

Abstract

Introduction

Conclusions

References

Tables

Figures

◀

▶

◀

▶

Back

Close

Full Screen / Esc

Printer-friendly Version

Interactive Discussion



neous distribution of supposed crustal conductors found by former studies. Comparing several findings of different authors (see Tezkan et al., 1992; Schnegg, 1998; Gurk and Schnegg, 2001, and references within) with the distribution pattern of Carboniferous and Permian sediment deposit areas before the alpine orogeny (Pfiffner, 2010) a high coincidence is deducible. Carbon-bearing metasediments serve as a C-reservoir and are most likely the basis for the existence of graphite networks on shear-horizons (Nover et al., 2005). Evidence for enhanced coalification can be seen in the anthracite bearing layers found in many regions of the detected crustal conductor (e.g. Zone Houlli re and Black Forest). In the case of the Brian onnais, laboratory measurements directly assigned the high conductivity to the presence of carbon on grain boundaries (Losito et al., 2001), visible graphite like requested from several authors (e.g. Yardley and Valley, 1997). The electromagnetic strike direction of  $\sim N 30^\circ E$  beneath the Black Forest is seen to be related to the macroscopic strike direction of Carboniferous and Permian transform faults on the carbon-bearing crustal layers (Edel and Fluck, 1989) and fits well into the above mentioned findings on graphite networks.

The most important wide-angle reflection and refraction seismic cross-sections in the Western Alps, the focus area in this study, are the ECORS-CROP (Bernabini et al., 2003) and NRP-20-WEST lines (Escher et al., 1997). Electromagnetic and seismic results are not generally attributable to exactly the same geologic structure because the derived models are determined by physical properties (seismic velocities and electric resistivity) that are not linked by an universal law (Mu oz et al., 2010). But in this case we compare a structure (here the crustal conductor) as a representative layer of the crust that can be imaged by electromagnetics with the general values obtained by seismics for the Earth's crust. Therefore from seismic results independent modeling of the crustal structures revealed dipping directions and angles ( $10.1^\circ S-SE$ , see Sect. 4.3) of the crustal conductors of the same order like values for the crust mantle boundary ( $6-12^\circ SE$  (western Alps) to  $NE$  (eastern Alps)) derived from former refraction seismic measurements in the central Alpine mountains (see Scarascia and Cassinis, 1997 and

Kummerow, 2003 for a good overview). They fit well into the 2-D structure of the above mentioned seismic profiles in the western Alps.

The second important feature in the model is the mantle conductor. As shown in Figs. 6 to 11 a conductive mantle beneath the Alps is necessary for better data fitting.

5 On the one hand an anisotropic mantle is needed to explain MT data in the Black Forest but on the other hand this feature is not necessary in the Alps anymore. Nevertheless it is still possible that a higher conductive direction exists because we consider the course of the phase split of INNT (Fig. 8) as an overprinting effect of deep dipping lithospheric structures, potentially reaching mantle level.

10 The nature of the high upper mantle conductivity likewise remains under discussion. Considering the Hashin–Shtrikman upper bound of 2-phase mediums either the presence of small amounts (0.03%) of carbonatite melts (Gaillard et al., 2008) or water bearing melts (3%) (Tarits et al., 2004) or high amounts of hydrous olivin (Simpson and Tommasi, 2005) or even the mix of it are likely to be the cause for conductivities of  
15  $0.01 \text{ S m}^{-1}$ . We attribute the deeper lying top of the conductive mantle to lithospheric roots, subducted lithosphere determined by teleseismic tomography (Kissling et al., 2006), breaking the dominating conduction mechanism.

## 6 Conclusions

20 This first large scale electromagnetic study in the Western European Alps revealed the existence of crustal and mantle conductors beneath the mountain chain. 3-D forward modeling allowed us to achieve a reasonable model for the Western Alps. It successfully tested hypothesis concerning the influence of certain geological structures and allowed limiting the possibilities of sources of high conductivity in the crust. In detail, the existence of graphite is the only reasonable explication for the results in this study  
25 (see Sect. 5). The source of high conductivity in the mantle cannot be contained by this study mainly because of the lack of long period electric data at disturbed stations (Sect. 5).

Title Page

Abstract

Introduction

Conclusions

References

Tables

Figures

◀

▶

◀

▶

Back

Close

Full Screen / Esc

Printer-friendly Version

Interactive Discussion



## Alps conductivity

D. Al-Halbouni

Title Page

Abstract

Introduction

Conclusions

References

Tables

Figures

◀

▶

◀

▶

Back

Close

Full Screen / Esc

Printer-friendly Version

Interactive Discussion



We find a thicker lithosphere beneath the central part of the Western Alps. Similarly to the crust we regard mechanical interruption of conductive mantle structures as the principal cause for the deep LAB. In this context the reproduction of MT and GDS data for short and long periods at station INNT (Figs. 1, 8, 10 and 11) is crucial because of its distinguished location near the interruption boundary in the Valais. Regarding the general behavior of GDS and MT data on a large scale we conclude that the influence of highly conductive structures and their interruption is much higher than the influence of conductive sedimentary structures surrounding the alpine mountain chain. Consequently tectonic movements before the alpine orogeny are responsible for the evolution of these highly conductive structures augmenting their integrated conductivity well above that of tertiary sediments.

Electromagnetic anisotropy of  $A = 1.41$  striking  $N30^\circ E$  is confirmed for the northern crustal conductor (C1) beneath the Black Forest and is regarded as hidden but possibly still existent at a less degree beneath the boundary between the Helvetic and Penninic Nappes due to an overprinting effect of the dipping structures which have the same influence on phase splits. The same is regarded as plausible for the mantle conductor (MC) with  $A = 1.73$  striking  $N80\text{--}90^\circ E$ . Due to modeling restrictions of anisotropy regarding GDS parameters these values are derived only by MT and this is seen as a necessary implementation in future 3-D forward modelling codes. We consider it probable that the observed E–W electromagnetic strike of the mantle conductor as well as the NE strike in the crustal conductor beneath the Black Forest (Sect. 4.4) disappear because of interruption processes during alpine formation.

As a quintessence for the Earth's crust in the Alps we state that the paleogeographic distribution of land-masses and tectonic processes before the alpine orogeny is the basic background for the current distribution pattern of conductive structures. The near-equator position of the former Laurussia and later Pangaea continent was essential for the variscian development of coal-bearing sedimentary deposits (McCann, 2008). We attribute the electromagnetic strike direction of  $N30^\circ E$  beneath the Black Forest directly to graphite networks arising from Carboniferous and Permian transform

## Alps conductivity

D. Al-Halbouni

Title Page

Abstract

Introduction

Conclusions

References

Tables

Figures

◀

▶

◀

▶

Back

Close

Full Screen / Esc

Printer-friendly Version

Interactive Discussion



faults, reactivated during the alpine collision (Edel and Fluck, 1989). We believe that the formation of the Tethyan and Penninic Oceans and the alpine collision (Schmid et al., 2004) mechanically interrupted former continuous widespread conductors; the latter leading to breaking of graphite networks through fragmentation, dipping and lithosphere stacking beginning at depth around 13 km (compare Sect. 4.3). This is seen to be the principal cause for the interruption occurring beneath the Helvetic and Penninic Alps (Fig. 1).

Tracing the form and direction of these conductors with electromagnetic methods gives the opportunity to derive directions and strength (depths) of alpine thrusting. In this case a dominant  $10.1^\circ$  S–SE dipping of the northern crustal conductor beneath the Alps is revealed. Additionally it serves as a Supplement concerning the paleogeographical origin of specific parts or even terranes. Therefore we state that the heterogeneous distribution of crustal conductors, found nowadays in the Alps, are metamorphosed remains of large paleozoic sedimentary deposits that additionally prove the connection between geologic domains like the Briançonnais and European continent (Bucher et al., 2004). These findings could consequently be taken under consideration when explaining the existence of proposed crustal conductors in regions with similar tectonic evolution like the Pyrenees and the Betic cordillera (Ledo et al., 2000; Martí et al., 2004).

In summary the combination of GDS and MT is essential to derive a to a certain degree suitable 3-D forward model in a electromagnetically highly disturbed environment where the lack of MT data is compensated by GDS. The application of a combined modeling has been successful, providing far more information than a simple 2-D interpretation would do, although there are certain restrictions one has to consider when working with the 3-D forward code mentioned in Sect. 4.4. In this study we have been able not only to identify and characterize the nature of highly conductive crustal and mantle structures beneath the Western European Alps, but also to reveal new insights into the orogenic background and tectonic context, into which the conductors are embedded. This finally leads to a qualitative interpretation of quantitative geophysical re-

sults in relation to the geological evolution in the Alps (Sect. 4 and 5). Following studies should take advantage of these new insights, of the existing model and its' ideas and draw case sensitive conclusions in related EM studies and apply similar 3-D modeling ideas to reproduce data in tectonically related environments.

5 *Acknowledgements.* Without the help of the German (Forstrevier Oberwolfach-Süd and Murg-Laufenburg), Swiss (Forstrevier Innertkirchen) and Italian (Comunità Montana Valgrande, Comunità Collinare Intorno al Lago, Parco Nazionale Val Grande and Parco Nazionale Alta Valsesia) forest and national park administrations this study would not have been possible. Special thanks go to Friedemann Samrock for advices, Ulrich Einecke and Manfred Herden  
10 for “robust” assistance as well as all people of the University of Göttingen who helped in the survey, especially Karsten Bahr. Additionally I personally would like to thank the reviewers for their useful comments as well as Fernando Monteiro Dos Santos.

This Open Access Publication is funded by the University of Göttingen.

## References

- 15 Artemieva, I. M.: The continental lithosphere: reconciling thermal, seismic, and petrologic data, *Lithos*, 109, 23–46, available at: <http://linkinghub.elsevier.com/retrieve/pii/S0024493708002211>, 2009. 1033
- Bahr, K.: Interpretation of the magnetotelluric impedance tensor: regional induction and local telluric distortion, *J. Geophys.*, 62, 119–127, 1988. 1036
- 20 Bahr, K.: Geological noise in magnetotelluric data: a classification of distortion types, *Phys. Earth Planet. In.*, 66, 24–38, 1991. 1036
- Bahr, K.: Elektromagnetische Tiefenforschung und Tektonik: Ihre Verknüpfung über die Geometrie von Gemischen, Habilitation, Johann Wolfgang Goethe-Universität Frankfurt am Main, 1993. 1033
- 25 Bahr, K., Olsen, N., and Shankland, T. J.: On the combination of the magnetotelluric and the geomagnetic depthsounding method for resolving an electrical conductivity increase at 400 km depth, *Geophys. Res. Lett.*, 20, 2937–2940, 1993. 1044
- Bernabini, M., Nicolich, R., and Polino, R.: Seismic lines CROP-ECORS across the western Alps, *Mem. Deser. Carta Geol. d'It.* LXII, 89–96, 2003. 1048

Title Page

Abstract

Introduction

Conclusions

References

Tables

Figures



Back

Close

Full Screen / Esc

Printer-friendly Version

Interactive Discussion



## Alps conductivity

D. Al-Halbouni

Title Page

Abstract

Introduction

Conclusions

References

Tables

Figures

◀

▶

◀

▶

Back

Close

Full Screen / Esc

Printer-friendly Version

Interactive Discussion



- Bucher, S., Ulardic, C., Bousquet, R., Ceriani, S., Fügenschuh, B., Gouffon, Y., Schmid, S. M.: Tectonic evolution of the Briançonnais units along a transect (ECORS-CROP) through the Italian-French western Alps, *Eclogae Geol. Helv.*, 97, 321–345, 2004. 1051
- Cagniard, L.: Basic theory of the magneto-telluric method of geophysical prospecting, *Geophysics*, 18, 605–635, 1953. 1036
- Caldwell, T. G., Bibby, H. M., and Brown, C.: The magnetotelluric phase tensor, *Geophys. J. Int.*, 158, 457–469, 2004. 1036, 1041
- Coward, M. and Dietrich, D.: Alpine tectonics-an overview, Geological Society London Special Publications, 45, 1–29, 1989. 1058
- Edel, J. B. and Fluck, P.: The upper Rhenish Shield basement (Vosges, Upper Rhinegraben and Schwarzwald): main structural features deduced from magnetic, gravimetric and geological data, *Tectonophysics*, 169, 303–316, 1989. 1048, 1051, 1069
- Egbert, G. D. and Booker, J. R.: Robust estimation of geomagnetic transfer functions, *Geophys. J. Roy. Astr. S.*, 87, 173–194, 1986. 1034, 1038
- Eisel, M. and Haak, V.: Macro-anisotropy of the electrical conductivity of the crust: a magnetotelluric study of the German Continental Deep Drilling site (KTB), *Geophys. J. Int.*, 136, 109–122, 1999. 1036
- Escher, A., Hunziker, J. C., Marthaler, M., Masson, H., Sartori, M., and Steck, A.: Geologic framework and structural evolution of the western Swiss-Italian Alps, in: *Deep Structure of the Swiss Alps: Results of NRP*, Birkhäuser Verlag, Basel, 205–221, 1997. 1048
- Gaillard, F., Malki, M., Iacono-Marziano, G., Pichavant, M., and Scaillet, B.: Carbonatite melts and electrical conductivity in the asthenosphere, *Science*, 322, 1363–1365, 2008. 1049
- Gatzemeier, A. and Moorkamp, M.: 3-D modelling of electrical anisotropy from electromagnetic array data: hypothesis testing for different upper mantle conduction mechanisms, *Phys. Earth Planet. In.*, 149, 225–242, 2005. 1045
- Groom, R. W. and Bahr, K.: Corrections for near surface effects: decomposition of the magnetotelluric impedance tensor and scaling corrections for regional resistivities: a tutorial, *Surv. Geophys.*, 13, 341–379, 1992. 1036
- Gurk, M.: Magnetic distortion of GDS transfer functions: an example from the Penninic Alps of eastern Switzerland revealing a crustal conductor, *Earth, Planets Space*, 51, 1023–1034, 1999. 1041
- Gurk, M.: On the distribution of the electrical conductivity in the Central Alps, 35 – *Géophysique, Matériaux pour la Géologie de la Suisse*, Imprimeries Centrales Neuchâtel S.A., 2000. 1033

## Alps conductivity

D. Al-Halbouni

Title Page

Abstract

Introduction

Conclusions

References

Tables

Figures

◀

▶

◀

▶

Back

Close

Full Screen / Esc

Printer-friendly Version

Interactive Discussion



- Gurk, M. and Schnegg, P. A.: Anomalous directional behaviour of the real parts of the induction arrows in the eastern Alps: tectonic and palaeogeographic implications, *Ann. Geofis.*, 44, 659–669, 2001. 1041, 1048
- Heinson, G.: Electromagnetic studies of the lithosphere and asthenosphere, *Surv. Geophys.*, 20, 229–255, 1999. 1042
- Illies, J. H.: The Rhine graben rift system-plate tectonics and transform faulting, *Surv. Geophys.*, 1, 27–60, 1972. 1042
- Jones, A. G. and Groom, R. W.: Strike-angle determination from the magnetotelluric impedance tensor in the presence of noise and local distortion: rotate at your peril!, *Geophys. J. Int.*, 113, 524–534, 1993. 1036
- Jones, A. G., Plomerova, J., Korja, T., Sodoudi, F., and Spakman, W.: Europe from the bottom up: a statistical examination of the central and northern European lithosphere-asthenosphere boundary from comparing seismological and electromagnetic observations, *Lithos*, 120, 14–29, 2010. 1033, 1042
- Kemmerle, K.: Magnetotellurik am Alpen-Nordrand mit Diskussion der lokalen Effekte und Darstellung einer Einzeleffekt-Auswertung, Ph.D. thesis, Ludwig-Maximilians-Universität, München, 1977. 1033
- Kissling, E., Schmid, S. M., Lippitsch, R., Ansonge, J., and Fuegensschuh, B.: Lithosphere structure and tectonic evolution of the Alpine arc: new evidence from high-resolution teleseismic tomography, *Geol. Soc. London Memoirs*, 32, 129–145, 2006. 1049
- Korja, T.: How is the European Lithosphere imaged by Magnetotellurics?, *Surv. Geophys.*, 28, 239–272, 2007. 1033, 1040
- Kummerow, J.: Strukturuntersuchungen in den Ostalpen anhand des teleseismischen TRANSALP-Datensatzes, Ph.D. thesis, Freie Universität Berlin, 2003. 1049
- Larsen, J. C., Mackie, R. L., Fiordelisi, A., Manzella, A., Rieven, S.: Robust Processing for Removing Train Signals from Magnetotelluric Data in Central Italy, *Proceedings of the World Geothermal Congress*, 2, 903–908, 1995. 1038
- Ledo, J., Ayala, C., Pous, J., Queralt, P., Marcuello, A., and Muñoz, J. A.: New geophysical constraints on the deep structure of the Pyrenees, *Geophys. Res. Lett.*, 27, 1027–1040, 2000. 1051
- Leibecker, J., Gatzemeier, A., Höning, M., Kuras, O., and Soyer, W.: Evidence of electrical anisotropic structures in the lower crust and the upper mantle beneath the Rhenish Shield, *Earth Planet. Sc. Lett.*, 202, 289–302, 2002. 1033

## Alps conductivity

D. Al-Halbouni

Title Page

Abstract

Introduction

Conclusions

References

Tables

Figures

◀

▶

◀

▶

Back

Close

Full Screen / Esc

Printer-friendly Version

Interactive Discussion



- Losito, G., Schnegg, P. A., Lambelet, C., Viti, C., and Trova, A.: Microscopic scale conductivity as explanation of magnetotelluric results from the Alps of Western Switzerland, *Geophys. J. Int.*, 147, 602–609, 2001. 1048
- Mackie, R. L. and Booker, J.: Documentation for mtd3fwd and d3-to-mt, GSY-USA Inc., San Francisco, CA, User Documentation, 1999. 1040, 1045, 1046
- Martí, A., Queralt, P., and Roca, E. Geoelectric dimensionality in complex geological areas: application to the Spanish Betic Chain, *Geophys. J. Int.*, 157, 961–974, 2004. 1051
- McCann, T.: *The Geology of Central Europe: Precambrian and Palaeozoic*, Vol. 1, The Geological Society London, London, 2008. 1050
- Medimap Group and Loubrieu, B. Mascle. J.: Morpho-bathymetry of the mediterranean sea, CIESM/Ifremer edition, 2 maps at 1/2 000 000, 2005. 1043
- Monteiro, F. A., Nolasco, M., and Pous, J.: Coast effects on magnetic and magnetotelluric transfer functions and their correction: application to MT soundings carried out in SW Iberia, *Earth Planet. Sc. Lett.*, 186, 283–295, 2001. 1043
- Muñoz, G., Bauer, K., Moeck, I., Schulze, A., and Ritter, O.: Exploring the GroßSchönebeck (Germany) geothermal site using a statistical joint interpretation of magnetotelluric and seismic tomography models, *Geothermics*, 39, 35–45, available at: <http://linkinghub.elsevier.com/retrieve/pii/S0375650509000765>, 2010. 1048
- Nover, G., Stoll, J. B., and von der Gönna, J.: Promotion of graphite formation by tectonic stress—a laboratory experiment, *Geophys. J. Int.*, 160, 1059–1067, 2005. 1047, 1048
- Pádua, M. B., Padilha, A. L., and Vitorello, I.: Disturbances on magnetotelluric data due to DC electrified railway: a case study from southeastern Brazil, *Earth, Planets Space*, 54, 591–596, 2002. 1038
- Parkinson, W. D.: Directions of rapid geomagnetic fluctuations, *Geophys. J. Roy. Astr. S.*, 2, 1–14, 1959. 1037, 1043
- Pfiffner, O. A.: *Geologie der Alpen*, Haupt UTB, Bern, Stuttgart, Wien, 2010. 1048
- Routh, P. S. and Oldenburg, D. W.: Inversion of controlled source audio-frequency magnetotellurics data for a horizontally layered earth, *Geophysics*, 64, 1689–1697, 1999. 1039
- Scarascia, S. and Cassinis, R.: Crustal structures in the central-eastern Alpine sector: a revision of the available DSS data, *Tectonophysics*, 271, 157–188, available at: <http://linkinghub.elsevier.com/retrieve/pii/S0040195196002065>, 1997. 1048
- Schmid, S. M. and Kissling, E.: The arc of the western Alps in the light of geophysical data on deep crustal structure, *Tectonics*, 19, 62–85, 2000. 1033

## Alps conductivity

D. Al-Halbouni

Title Page

Abstract

Introduction

Conclusions

References

Tables

Figures

◀

▶

◀

▶

Back

Close

Full Screen / Esc

Printer-friendly Version

Interactive Discussion



- Schmid, S. M., Fügenschuh, B., Kissling, E., and Schuster, R.: Tectonic map and overall architecture of the Alpine orogen, *Ecolgae Geologicae Helvetiae*, 97, 93–117, 2004. 1051, 1058
- Schmucker, U.: Anomalies of Geomagnetic Variations in the Southwestern United States, University of California Press, USA, 1970. 1036
- Schmucker, U. and Tezkan, B.: 20 Jahre elektromagnetische Tiefenforschung im Rheingraben – eine Zusammenfassung mit Ausblick auf neuere Ergebnisse, in: Prot. 12. Koll. “Elektromagnetische Tiefenforschung”, edited by: Haak, V. and Homilius, J., Königstein im Taunus, 1988. 1033, 1042
- Schnegg, P. A.: The magnetotelluric survey of the Penninic Alps of Valais, Vol. 32 – Géoph. of Matériaux pour la Géologie de la Suisse, Imprimeries Centrales Neuchâtel S.A., 1998. 1033, 1044, 1048
- Schwarz, G.: Electrical conductivity of the Earth’s crust and upper mantle, *Surv. Geophys.*, 11, 133–161, 1990. 1047
- Simpson, F.: Stress and seismicity in the lower continental crust: a challenge to simple ductility and implications for electrical conductivity mechanisms, *Surv. Geophys.*, 20, 201–227, 1999. 1047
- Simpson, F. and Bahr, K.: *Practical Magnetotellurics*, Cambridge University Press, Cambridge, 2005. 1036, 1043, 1069
- Simpson, F. and Tommasi, A.: Hydrogen diffusivity and electrical anisotropy of a peridotite mantle, *Geophys. J. Int.*, 160, 1092–1102, 2005. 1043, 1049
- Szarka, L.: Geophysical aspects of man-made electromagnetic noise in the earth—a review, *Surv. Geophys.*, 9, 287–318, 1988. 1039
- Tarits, P., Hautot, S., and Perrier, F.: Water in the mantle: results from electrical conductivity beneath the French Alps, *Geophys. Res. Lett.*, 31, L06612, doi:10.1029/2003GL019277, 2004. 1049
- Tezkan, B., Červ, V., and Pek, J.: Resolution of anisotropic and shielded highly conductive layers using 2-D electromagnetic modelling in the Rhine Graben and Black Forest, *Phys. Earth Planet. In.*, 74, 159–172, 1992. 1042, 1045, 1048
- Tikhonov, A. N.: The determination of the electrical properties of deep layers of the Earth’s crust, *Dokl. Acad. Nauk. SSR*, 73, 295–297, 1950. 1036
- Waff, H. S.: Theoretical considerations of electrical conductivity in a partially molten mantle and implications for geothermometry, *J. Geophys. Res.*, 79, 4003–4010, 1974. 1047

## Alps conductivity

D. Al-Halbouni

[Title Page](#)[Abstract](#)[Introduction](#)[Conclusions](#)[References](#)[Tables](#)[Figures](#)[Back](#)[Close](#)[Full Screen / Esc](#)[Printer-friendly Version](#)[Interactive Discussion](#)

Wannamaker, P. E.: Comment on “The petrologic case for a dry lower crust” by Bruce WD Yardley and John W. Valley, *J. Geophys. Res.*, 105, 6057–6064, 2000. 1047

Wannamaker, P. E.: Anisotropy versus heterogeneity in continental solid earth electromagnetic studies: fundamental response characteristics and implications for physicochemical state, *Surv. Geophys.*, 26, 733–765, 2005. 1040

Weidelt, P.: The inverse problem of geomagnetic induction, *Z. Geophys.*, 38, 257–290, 1972. 1036

Wiese, H.: Geomagnetische Tiefentellurik Teil II: die Streichrichtung der Untergrundstrukturen des elektrischen Widerstandes, erschlossen aus geomagnetischen Variationen, *Pure Appl. Geophys.*, 52, 83–103, 1962. 1037

Yardley, B. W. D. and Valley, J. W.: The petrologic case for a dry lower crust, *J. Geophys. Res.*, 102, 12173–12186, 1997. 1047, 1048

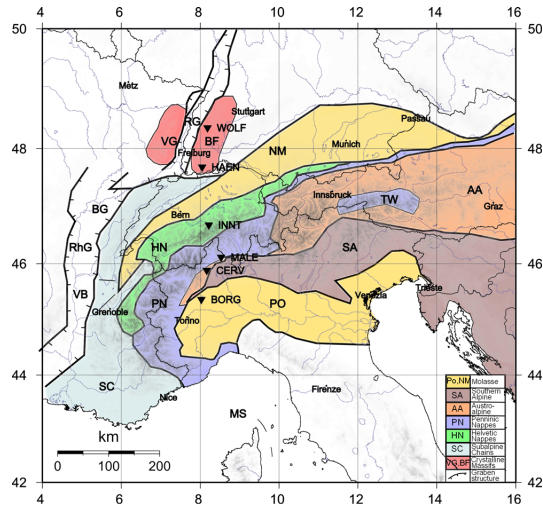


**Fig. 1.** Map showing the simplified tectonic regimes of the European Alps and surroundings as well as the location of the measurement stations along the N–S cross-section through the Western Alps. Latitude is given in degrees north and longitude in degrees east. Areas with the same color belong to the same tectonic regime. West and northwest of the Alpine arc the European Cenozoic rift system is sketched with its graben and basins: RG – Rhein Graben, RhG – Rhône Graben, BG – Bresse Graben and VB – Valence Basin. Surrounding the Alps in the west there are the Subalpine chains including the jura mountains (SC). In the Swiss, German and French part north and west of the alpine thrust the Northern and Western Molasse (NM) can be found whereas in the Italian part a sedimentary basin, the Po-basin (PO) is formed. Two highly crystalline zones can be found on both sides of the Rhine Graben, the Vosges (VG) and the Black Forest (BF). The main tectonic units of the Alpine mountain chain are the Helvetic Nappes (HN), the Penninic Nappes (PN), the Austroalpine (AA) and the Southern Alps (SA). In the Austroalpine regime a small area called Tauern Window (TW) allows a glance into the Penninic basement. The Mediterranean Sea (MS) forms the south border of the (visible) Western Alps. The map is drawn with information from Coward and Dietrich (1989) and Schmid et al. (2004).

Title Page

Abstract Introduction

Conclusions References

Tables Figures

◀ ▶

◀ ▶

Back Close

Full Screen / Esc

Printer-friendly Version

Interactive Discussion



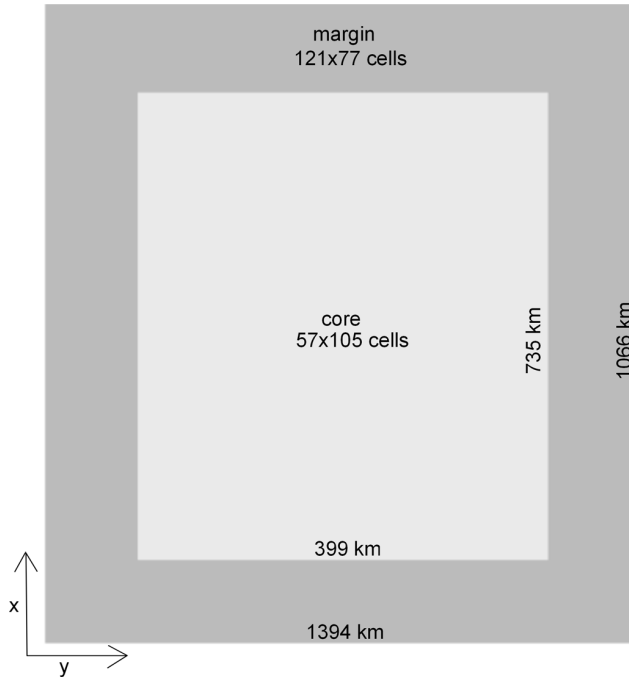


**Fig. 2.** XY-plane of the 3-D forward model developed in this study. The dimensions and cell numbers are indicated in the figure. The vertical ( $Z$ ) dimension is 34 levels with gradually increasing thickness up to a depth of 780 km. Additionally 10 air-layers ( $-Z$ ) are included in the model boundaries to achieve convergent results. The thickness of the levels can be deduced from the display of the model result in Fig. 3.

Title Page

Abstract

Introduction

Conclusions

References

Tables

Figures

◀

▶

◀

▶

Back

Close

Full Screen / Esc

Printer-friendly Version

Interactive Discussion



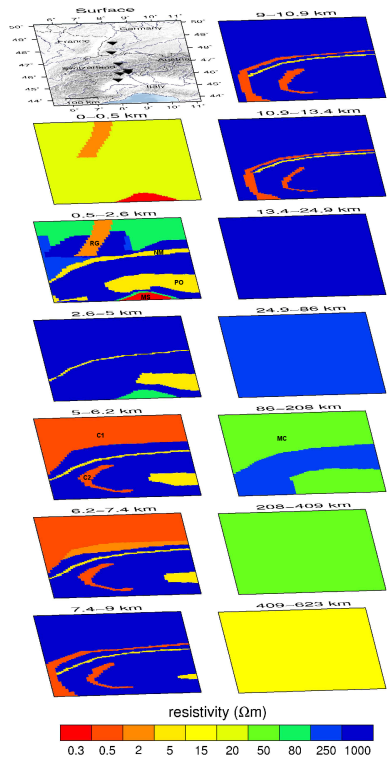


**Fig. 3.** 3-D forward model (735 km × 399 km) with best fit of observed GDS and MT data. Top layer represents the surface with inverted black triangles indicating the location of the measurement stations used for this study. From N to S these are WOLF, HAEN, INNT, MALE, VALG, CERV and BORG. The main features of the layers are the interruption of the northern, western (C1) and Briançonnais (C2) crustal conductors (red) and a deeper boundary between the lithosphere (blue) and asthenosphere (green) beneath the central part of the Western Alps. Additional relevant structures are the Po basin (PO), northern Molasse (NM), Rhine Graben (RG) as well as the Mediterranean Sea and Sediments (MS).

Title Page

Abstract

Introduction

Conclusions

References

Tables

Figures

◀

▶

◀

▶

Back

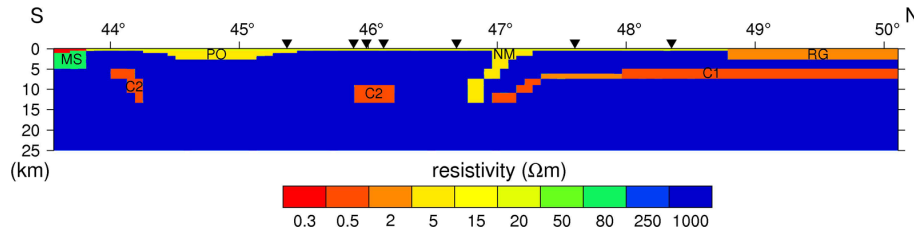
Close

Full Screen / Esc

Printer-friendly Version

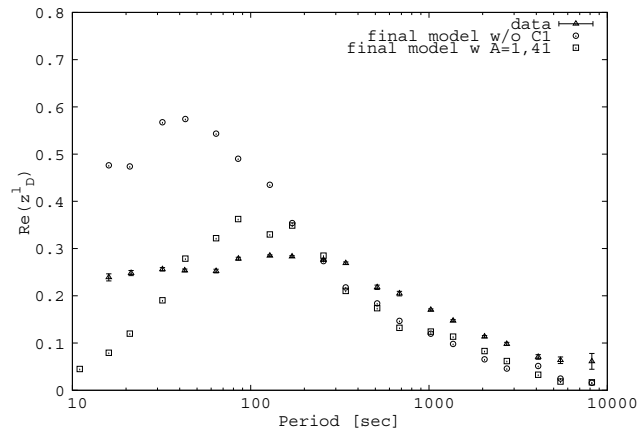
Interactive Discussion





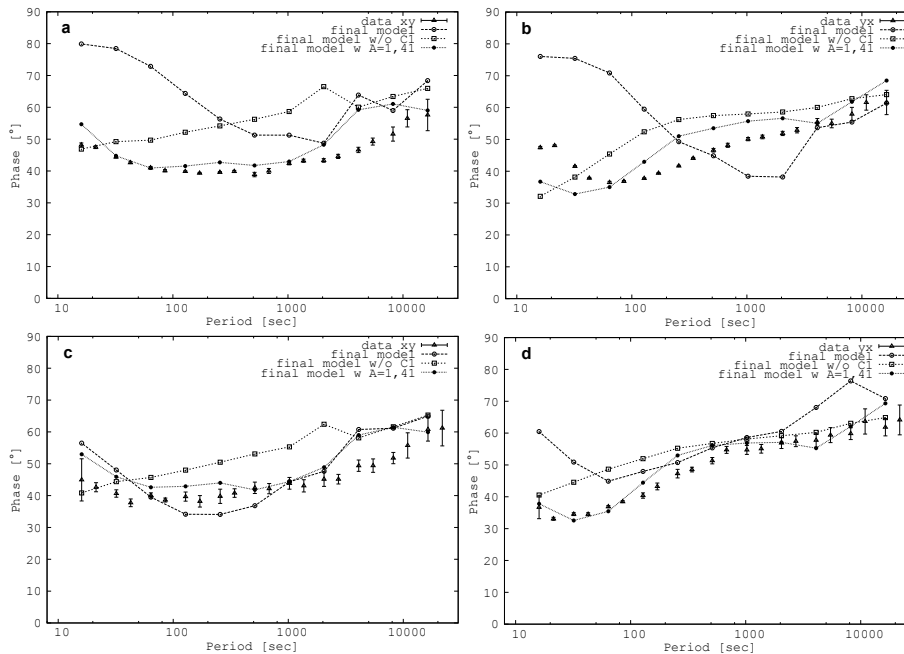
**Fig. 4.** 2-D N-S slice at 8.08° E through the first 25 km of the crust in the model. The cross-section refers to the approximate line on which the stations indicated by inverted black triangles are projected. The important structures which are embedded in a crystalline environment are here from left to right: MS – Mediterranean Sea and Sediments, C2 – Slices of Briançonnais crustal conductor, PO – Po basin, NM – northern Molasse, C1 – northern dipping crustal conductor and RG – Rhine Graben.

[Title Page](#)
[Abstract](#)
[Introduction](#)
[Conclusions](#)
[References](#)
[Tables](#)
[Figures](#)
[◀](#)
[▶](#)
[◀](#)
[▶](#)
[Back](#)
[Close](#)
[Full Screen / Esc](#)
[Printer-friendly Version](#)
[Interactive Discussion](#)

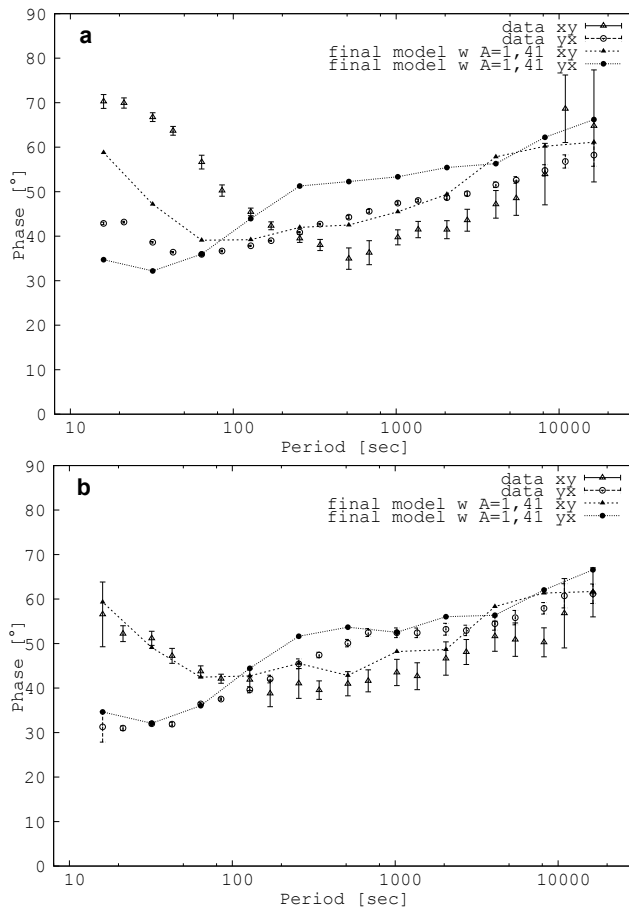
**Fig. 5.** Local induction  $z_D^1$  for station WOLF in the Black Forest. C1 is needed below the Black Forest to explain the low values at short periods. Model w/o C1 means that the resistivity of conductor C1 was equalized to the  $1000\ \Omega\text{m}$  crystalline background. Sediments of the N–S trending Rhine Graben produce high local induction in  $B_x$  which are levelled by the crustal conductor.

[Title Page](#)
[Abstract](#)
[Introduction](#)
[Conclusions](#)
[References](#)
[Tables](#)
[Figures](#)
[⏪](#)
[⏩](#)
[◀](#)
[▶](#)
[Back](#)
[Close](#)
[Full Screen / Esc](#)
[Printer-friendly Version](#)
[Interactive Discussion](#)

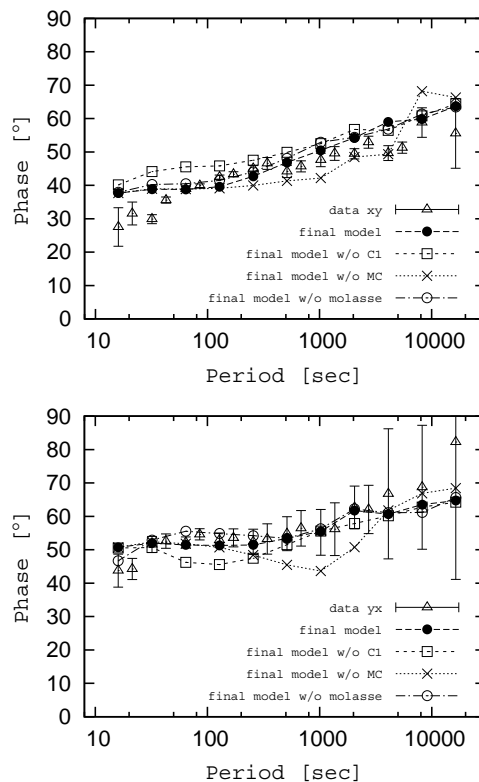



**Fig. 6.** Unrotated MT-Phases data and model (dashed lines) for station WOLF (**a** and **b**) and HAEN (**c** and **d**) in the Black Forest region. Top right corner indicates the polarization  $xy$  or  $yx$ . The final model can't explain the phase data sufficiently because of the modeling restrictions mentioned in Sect. 5. A model without the C1 neither is suited but the final model with an anisotropic crustal conductor ( $A = 1.41$ ) and an anisotropic mantle conductor ( $A = 1.73$ ) is able to reproduce the data in a reasonable manner.

[Title Page](#)
[Abstract](#)
[Introduction](#)
[Conclusions](#)
[References](#)
[Tables](#)
[Figures](#)
[◀](#)
[▶](#)
[◀](#)
[▶](#)
[Back](#)
[Close](#)
[Full Screen / Esc](#)
[Printer-friendly Version](#)
[Interactive Discussion](#)

**Fig. 7.** 30° clockwise rotated MT-Phases data and model (dashed lines) for stations WOLF (a) and HAEN (b) in the Black Forest region. The final model with an anisotropic C1 and an anisotropic MC fits well both polarizations.



**Fig. 8.** Unrotated MT-Phases data and model (dashed lines) for station INNT in the Valais region. A strong phase split for short and middle periods is observable, modeled by the dipping crustal conductor and dipping Molasse layer (Figs. 4 and 5). Here anisotropy both of the C1 and MC is not needed anymore, although it might exist at a smaller degree. The dipping layers produce a very well fit and this is regarded as a proof of lithosphere stacking which could be responsible for the interruption of conductors and the vanishing anisotropy (see Sect. 5).

Title Page

Abstract

Introduction

Conclusions

References

Tables

Figures

◀

▶

◀

▶

Back

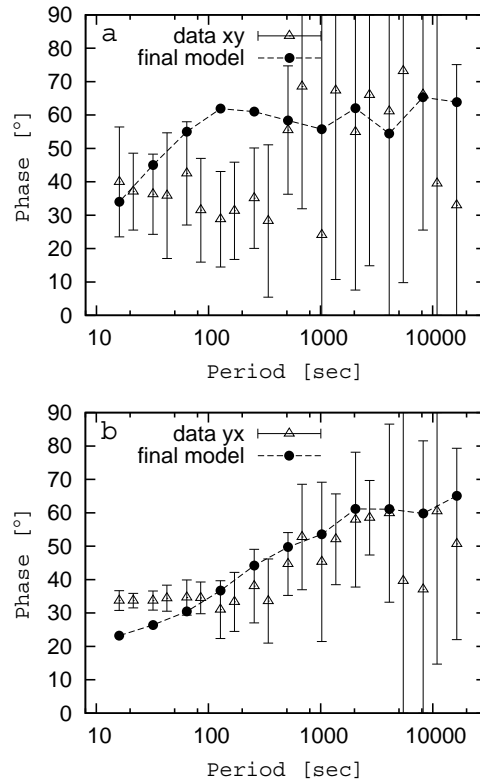
Close

Full Screen / Esc

Printer-friendly Version

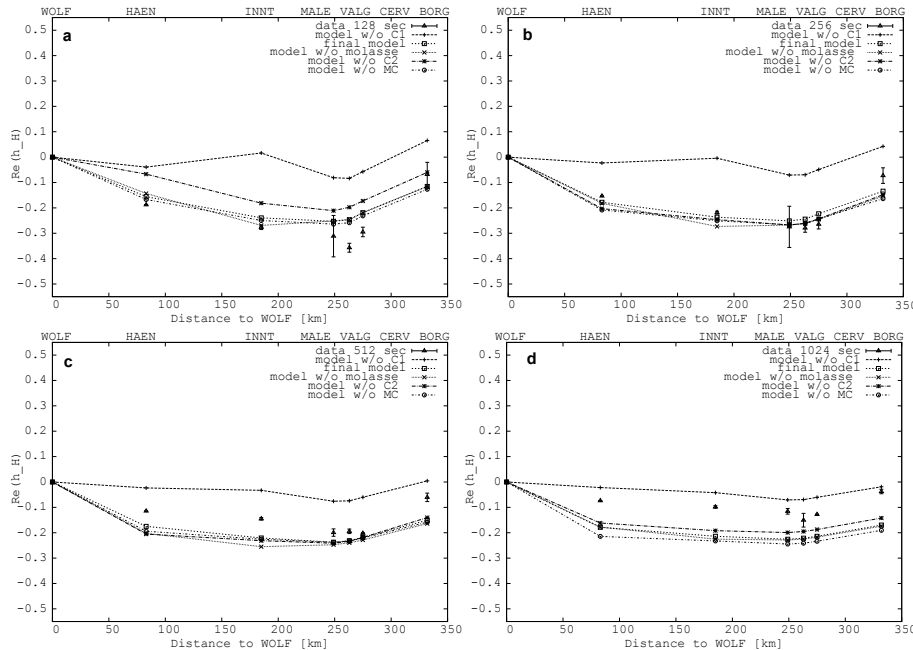
Interactive Discussion





**Fig. 9.** Unrotated MT-Phases data for both polarizations ( $xy$  in graph **a** and  $yx$  in graph **b**) and final model answer (dashed lines) for station BORG in the Po basin. The recovery of the highly disturbed electric data by Remote Reference leads to a better fit of the model for the  $yx$  polarization, but still the errors are too high to achieve a more reliable result.

[Title Page](#)
[Abstract](#)
[Introduction](#)
[Conclusions](#)
[References](#)
[Tables](#)
[Figures](#)
[◀](#)
[▶](#)
[◀](#)
[▶](#)
[Back](#)
[Close](#)
[Full Screen / Esc](#)
[Printer-friendly Version](#)
[Interactive Discussion](#)

**Fig. 10.** Values of the real part of  $h_H$  for data and model along the N–S profile with reference to WOLF. Different graphs show different periods indicated in the top right corner of the respective diagram. Top x-axis shows names of the stations. Lower x-axis indicates the distance from WOLF along a projected N–S line between WOLF and BORG (Fig. 1). Several models are compared with the results of the final model. Model w/o  $xy$  means that the resistivity of conductor  $xy$  was equalized to the resistivity of the background (conductor obviously disappears). A model without C1 can never explain the  $h_H$  trends and a missing MC shifts the whole results for longer periods (e.g. graph **d**) whereas other structures have only local influence (e.g. Molasse on INNNT, graph **b**). The observable reasonable fit shows that the final model (Figs. 4 and 5) can explain the large-scale GDS results in the Western European Alps by introducing dipping and interrupted conductors.

Title Page

Abstract

Introduction

Conclusions

References

Tables

Figures

◀

▶

◀

▶

Back

Close

Full Screen / Esc

Printer-friendly Version

Interactive Discussion



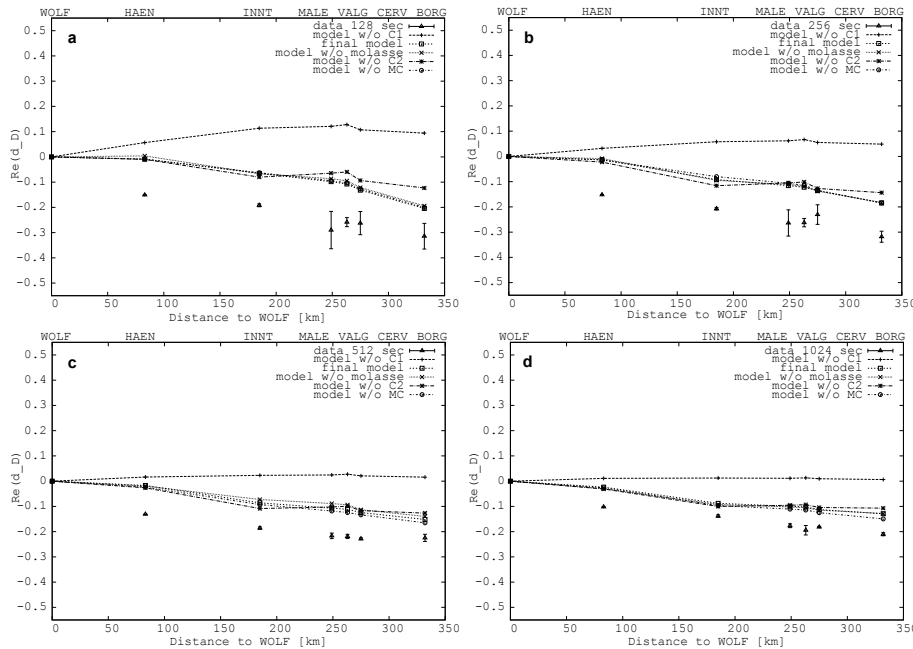


**Fig. 11.** Values of the real part of  $d_D$  for data and model (dashed lines) along the N–S profile with reference to WOLF. Different graphs show different periods indicated in the top right corner of the respective diagram. Top x axis shows names of the stations. Lower x axis indicates the distance from WOLF along a projected N–S line between WOLF and BORG (Fig. 1). Although the model fit is poorer than for the  $h_H$  component it proves the applicability of the final model (Figs. 4 and 5) and the relevance of the western and Briançonnais crustal conductor (C1 and C2).

Title Page

Abstract

Introduction

Conclusions

References

Tables

Figures

⏪

⏩

◀

▶

Back

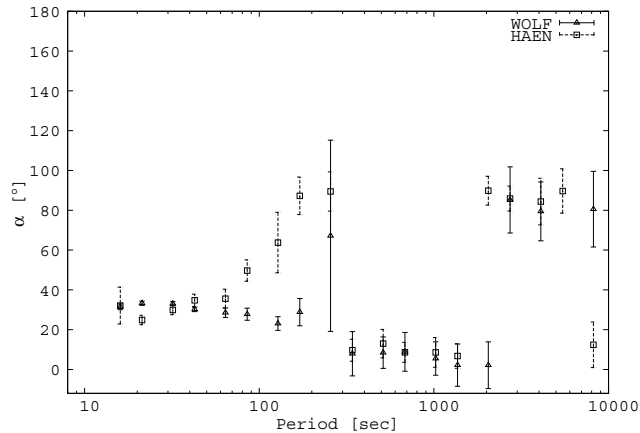
Close

Full Screen / Esc

Printer-friendly Version

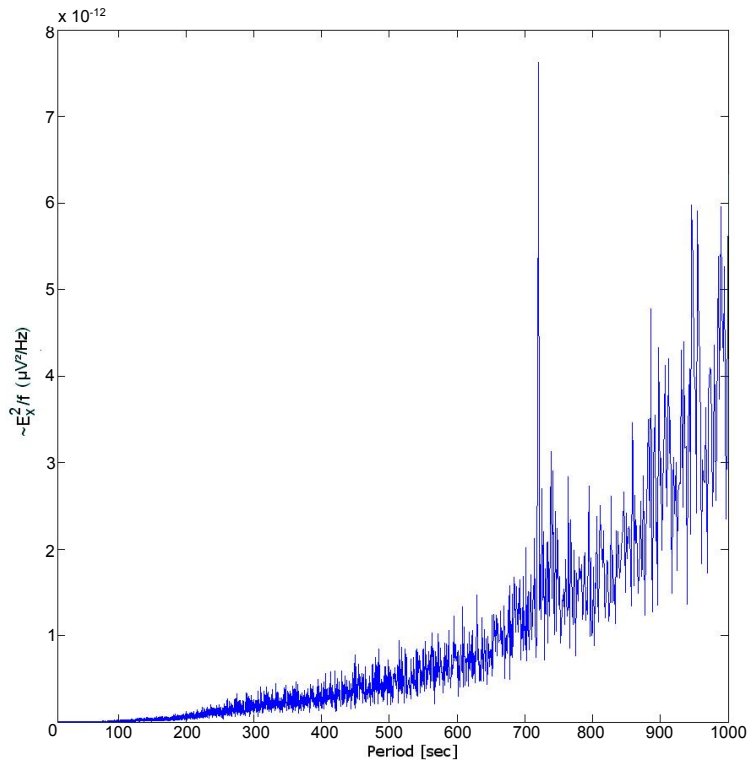
Interactive Discussion





**Fig. 12.** Phase-sensitive electromagnetic strike of both stations in the Black Forest. A mean value around  $30^\circ$  is found and is related to macroscopic anisotropic structures represented by the Carboniferous and Permian transform faults (Edel and Fluck, 1989), Longer Periods reveal a dominant E-W electromagnetic strike taking into account the  $90^\circ$  ambiguity of magnetotellurics (Simpson and Bahr, 2005). Underdetermined periods are not shown.

[Title Page](#)
[Abstract](#)
[Introduction](#)
[Conclusions](#)
[References](#)
[Tables](#)
[Figures](#)
[◀](#)
[▶](#)
[◀](#)
[▶](#)
[Back](#)
[Close](#)
[Full Screen / Esc](#)
[Printer-friendly Version](#)
[Interactive Discussion](#)

**Fig. A1.** Powerspectrum of electric component  $E_x$  for station BORG. A high amplitude non-natural period (at around 730 s) can be observed but high noise peaks that lead to a sounding curve similar to Controlled Source MT (see Sect. 4.2) are not visible at all, being “shielded” by natural signals.

Title Page

Abstract

Introduction

Conclusions

References

Tables

Figures

◀

▶

◀

▶

Back

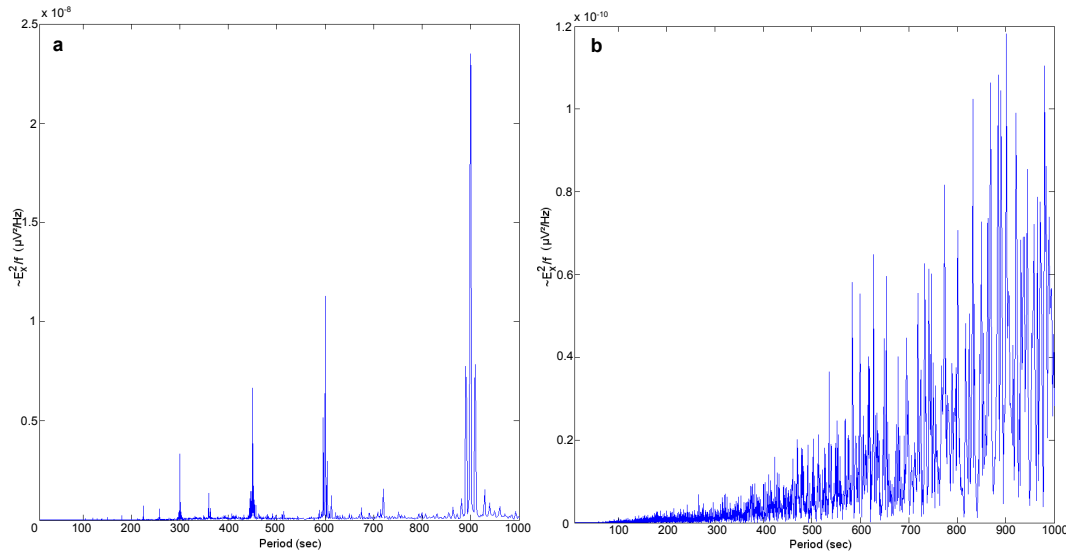
Close

Full Screen / Esc

Printer-friendly Version

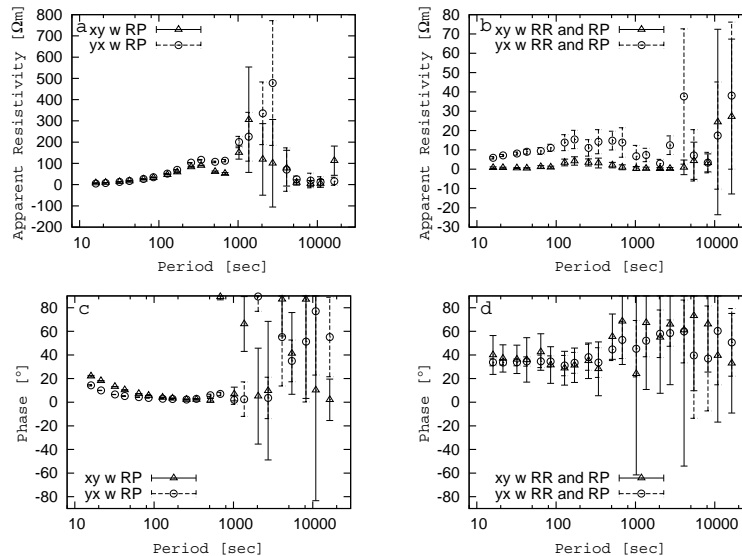
Interactive Discussion





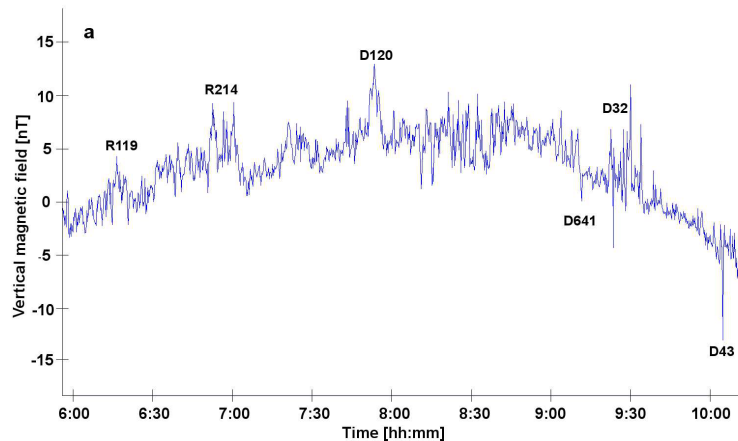
**Fig. B1a.** Powerspectrum of electric component  $E_x$  for station INNT. **(a)** shows high noise during day-time (04:00 a.m.–22:00 p.m.) whereas **(b)** indicates natural signals during night-time (22:00 p.m.–4:00 a.m.). Robust Processing and Remote Reference of the whole dataset with station WOLF yielded MT-results as good as that of the night data but with the advantage of a full period range. The signal-to-noise ratio was raised so that reliable results with coherences higher than 0.8. were achieved.

[Title Page](#)
[Abstract](#)
[Introduction](#)
[Conclusions](#)
[References](#)
[Tables](#)
[Figures](#)
[⏪](#)
[⏩](#)
[◀](#)
[▶](#)
[Back](#)
[Close](#)
[Full Screen / Esc](#)
[Printer-friendly Version](#)
[Interactive Discussion](#)

**Fig. B1b.** Apparent Resistivity (top) and phase (bottom) for the southernmost station BORG. **(a)** and **(c)** show the sounding curves of data processed robustly whereas **(b)** and **(d)** stand for the results after additional Remote Reference processing. **(a)** together with **(c)** is comparable to typical Controlled Source MT curves (see text for details) and spectra analysis gives no indication about the high artificial disturbances. Finally using a remote station (here WOLF) helps to recover the station at least partially.

[Title Page](#)
[Abstract](#)
[Introduction](#)
[Conclusions](#)
[References](#)
[Tables](#)
[Figures](#)
[◀](#)
[▶](#)
[◀](#)
[▶](#)
[Back](#)
[Close](#)
[Full Screen / Esc](#)
[Printer-friendly Version](#)
[Interactive Discussion](#)

**b**

Station/stop: ■ Malesco  
 Timetable: Departure 00:00:23:59 27.03.09 - 02.04.09 » [current time](#)

Time	Travel with	Timetable
06:19	R 119 Locarno FART	Malesco 06:19 - Villette (Vigezzo) 06:22 - Re 06:24 - Felsogno-Dissimo 06:27 - Camedo 06:39 - Intragna 06:56 - Cavigliano 07:00 - Ponte Brolla 07:07 - Locarno S. Antonio 07:12 - Locarno FART 07:18 Mo - Fr
06:51	R 214 Domodossola	Malesco 06:51 - Zornasco 06:53 - Prestinone 06:55 - S. Maria Maggiore 07:00 - Druogno 07:05 - Gagnone-Oressco 07:08 - Verigo 07:21 - Trontano 07:26 - Masera 07:36 - Domodossola 07:42 daily
07:49	D 120 Domodossola	Malesco 07:49 - Zornasco 07:50 - Prestinone 07:53 - S. Maria Maggiore 07:55 - Druogno 08:00 - Gagnone-Oressco 08:03 - Verigo 08:16 - Trontano 08:21 - Masera 08:31 - Domodossola 08:37 daily
08:53	R 231 Re	Malesco 08:53 - Villette (Vigezzo) 08:57 - Re 08:59 daily
09:11	D 32 Domodossola	Malesco 09:11 - Prestinone 09:14 - S. Maria Maggiore 09:17 - Druogno 09:21 - Trontano 09:41 - Masera 09:51 - Domodossola 09:56 daily
09:11	D 641 Locarno FART	Malesco 09:11 - Re 09:17 - Camedo 09:32 - Verfasio 09:41 - Intragna 09:50 - Ponte Brolla 10:01 - Locarno S. Antonio 10:06 - Locarno FART 10:10 25. Mar until 18. Oct 2009 daily
10:11	D 43 Locarno FART	Malesco 10:11 - Re 10:17 - Camedo 10:32 - Verfasio 10:42 - Intragna 10:51 -

Title Page

Abstract Introduction

Conclusions References

Tables Figures

◀ ▶

◀ ▶

Back Close

Full Screen / Esc

Printer-friendly Version

Interactive Discussion

Fig. B2. Caption on next page.



## Alps conductivity

D. Al-Halbouni

Title Page

Abstract

Introduction

Conclusions

References

Tables

Figures



Back

Close

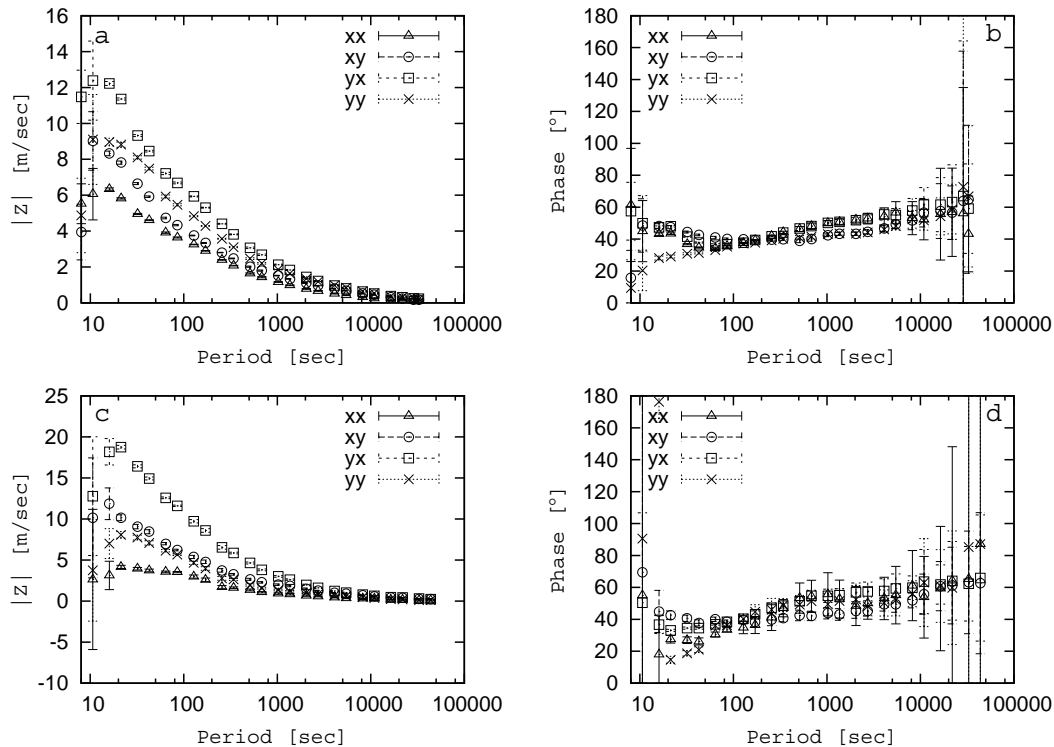
Full Screen / Esc

Printer-friendly Version

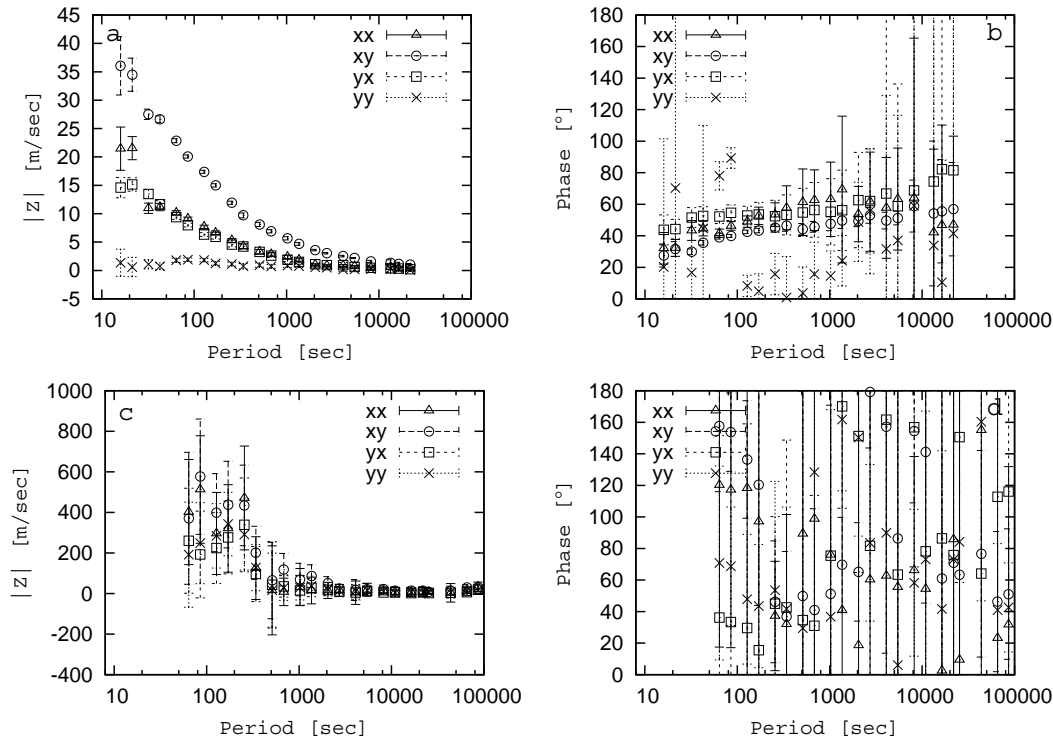
Interactive Discussion



**Fig. B2.** Near-distance magnetic influence of DC railways. **(a)** shows the vertical magnetic field component  $B_z$  for station MALE approximately 2 km away from the Italian village and train station Malesco. The amplitude of the variations is shown for the 1 April 2009. Marked peaks belong to certain trains found in the excerpt of the timetable **(b)**, downloaded on 13 March 2009 at 12:30 LT on <http://www.sbb.ch>.

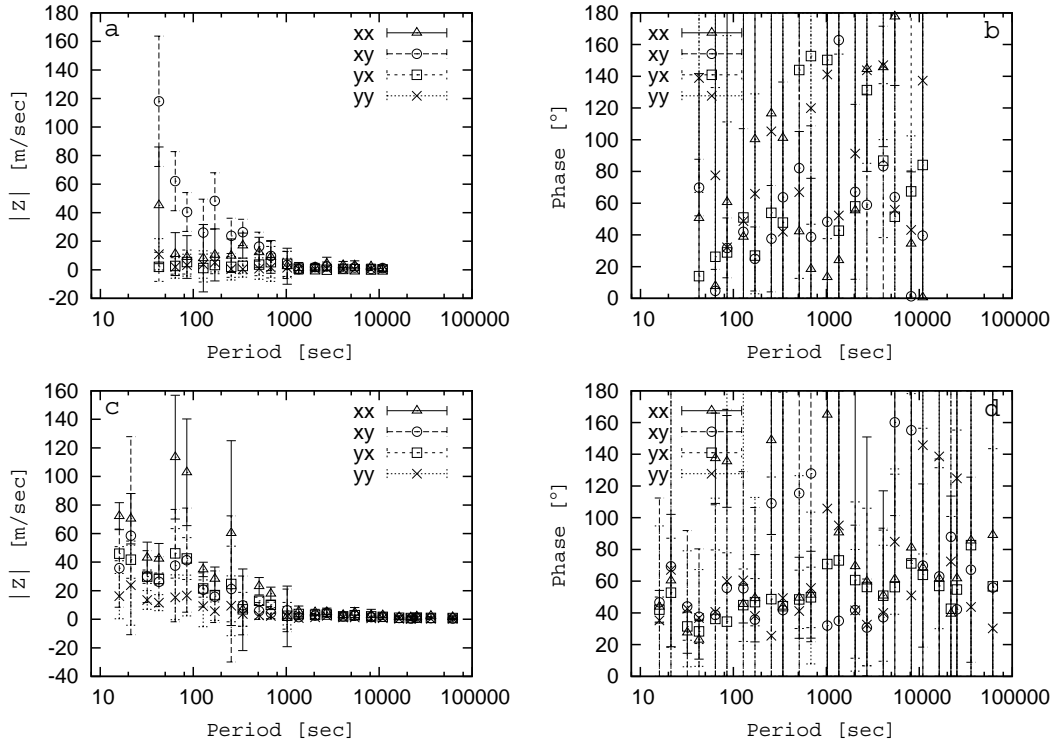


**Fig. C1.** Unrotated impedance tensor elements for stations WOLF (**a** and **b**) and HAEN (**c** and **d**) in the Black Forest region. Top right corner indicates the polarization. Both stations are included in the modeling.



**Fig. C2.** Unrotated impedance tensor elements for stations INNT (a and b) and MALE (c and d) in the Valais and Piemont region. Top right corner indicates the polarization. Only INNT is included in the model because MALE is electrically completely disturbed and not correctable.

[Title Page](#)
[Abstract](#)
[Introduction](#)
[Conclusions](#)
[References](#)
[Tables](#)
[Figures](#)
[◀](#)
[▶](#)
[◀](#)
[▶](#)
[Back](#)
[Close](#)
[Full Screen / Esc](#)
[Printer-friendly Version](#)
[Interactive Discussion](#)

**Fig. C3.** Unrotated impedance tensor elements for stations VALG (a and b) and CERV (c and d) in the Piemont region. Top right corner indicates the polarization. No station is included in the model because of the observable high disturbances.

Title Page

Abstract Introduction

Conclusions References

Tables Figures

◀ ▶

◀ ▶

Back Close

Full Screen / Esc

Printer-friendly Version

Interactive Discussion



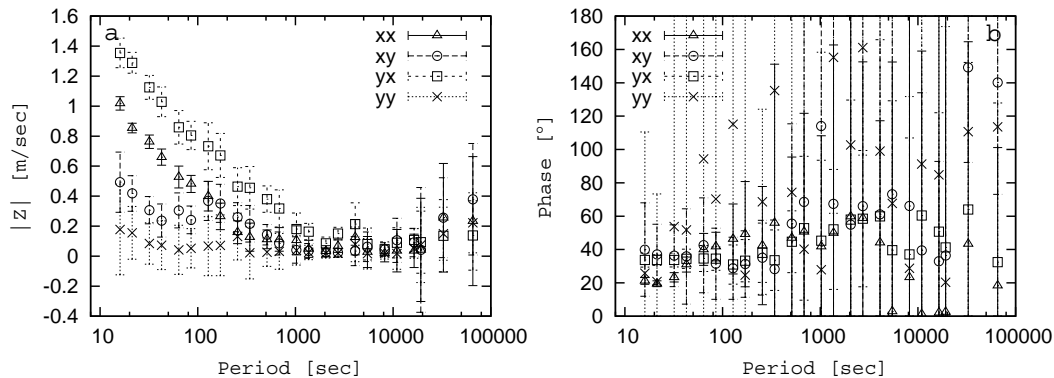


**Fig. C4.** Unrotated impedance tensor elements for station BORG (a and b) in the Po-basin. Top right corner indicates the polarization. After correction with RP and RR results of BORG are taken under consideration in the model.

[Title Page](#)
[Abstract](#)
[Introduction](#)
[Conclusions](#)
[References](#)
[Tables](#)
[Figures](#)
[◀](#)
[▶](#)
[◀](#)
[▶](#)
[Back](#)
[Close](#)
[Full Screen / Esc](#)
[Printer-friendly Version](#)
[Interactive Discussion](#)




**Fig. D1.** Measuring device RAP (bottom) used in this study. Together with a triaxial fluxgate magnetometer and Ag–AgCl electrodes the equipment was developed at the University of Göttingen. Snow cover (top) showed to be advantageous to reduce temperature related noise.

## SED

5, 1031–1079, 2013

### Alps conductivity

D. Al-Halbouni

Title Page

Abstract

Introduction

Conclusions

References

Tables

Figures

⏪

⏩

◀

▶

Back

Close

Full Screen / Esc

Printer-friendly Version

Interactive Discussion

